Available online at www.sciencedirect.com

ScienceDirect

Procedia Engineering 132 (2015) 342 – 349

Procedia Engineering

www.elsevier.com/locate/procedia

The Manufacturing Engineering Society International Conference, MESIC 2015

Recent approaches for the determination of forming limits by necking and fracture in sheet metal forming

M.B. Silva[a], A.J. Martínez-Donaire[b], G. Centeno[b], D. Morales-Palma[b], C. Vallellano[b,*], P.A.F. Martins[a]

[a] *Instituto Superior Técnico, Universidade de Lisboa, Av. Rovisco Pais, 1049-001 Lisbon, Portugal*
[b] *Dpt. Mechanical and Manufacturing Engineering, University of Seville, Av. de los Descubrimientos s/n, 41092 Sevilla, Spain*

Abstract

Forming limit diagrams (FLD's) are used to evaluate the workability of metal sheets. FLD's provide the failure locus at which plastic instability occurs and localized necking develops (commonly designated as the forming limit curve - FLC), and the failure loci at the onset of fracture by tension (FFL) or by in-plane shear (SFFL). The interest of metal formers in controlling localized necking is understandable because the consequence of plastic instability is an undesirable surface blemish in components. However, because under certain loading conditions fracture can precede necking in sheet metal forming processes, there is a growing interest in characterizing the forming limits by necking and fracture in the FLD's. This paper gathers together a number of recently developed methodologies for detecting the onset of local necking and fracture by in-plane tension or in-plane shear, and discusses their applicability to determine experimentally the FLC's, FFL's and SFFL's.

Peer-review under responsibility of the Scientific Committee of MESIC 2015

Keywords: Sheet metal forming; Failure; Necking; Fracture

1. Introduction

Fracture initiation and propagation in sheet metal forming is controlled by one of the following two mechanisms: (i) sheet thinning caused by localized necking along an inclined direction to the loading direction and (ii) sheet thinning caused by plastic flow without previous localized necking (Fig. 1).

* Corresponding author. Tel.: +34 954 487311; fax: +34 954 460475.
E-mail address: carpofor@us.es

Peer-review under responsibility of the Scientific Committee of MESIC 2015
doi:10.1016/j.proeng.2015.12.504

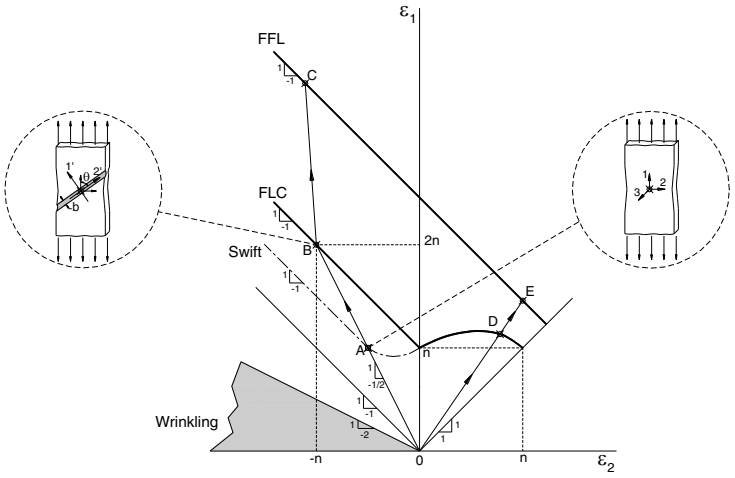

Fig. 1. Forming limit diagram (FLD) with the forming limit curve (FLC), the fracture forming limit line corresponding to crack opening by tension (FFL) and the onset of diffuse necking due to Swift [1].

In the early 1950's, Hill [2] associated the first fracture mechanism with plastic instability and, later in the mid 1960's, Marciniak [3] explained the experimental observations of strain localization in hydraulic bulging and punch stretching in the light of geometrical or structural non-homogeneity of the material. The mechanism of fracture with previous localized necking is schematically illustrated in the strain loading path OABC in Fig. 1, which is characterized by a sharp change towards near plane strain deformation after crossing the onset of necking (also known as the forming limit curve, FLC) at point B [1]. The FLC is commonly determined in accordance with the ISO 12004-2:2008 standard using Nakazima or Marciniak formability tests, for which bending effects are a priori negligible. In the current version of the standard, the onset of necking is estimated by means of a position-dependent methodology that requires analyzing the principal strain distribution on the sheet surface at a fixed and unique instant immediately before cracking. The practical application and limitations of this technique are comprehensively discussed by Hotz and Timm [4] and Martínez-Donaire et al. [5-7] and have been stimulating the development of alternative time-dependent methodologies to determine the FLC's. The new time-dependent methodologies are based on recent advances in optics and image processing and allow characterizing the onset of necking by analyzing the time evolution of strains at the fracture zone. The algorithms associated to these new time-dependent methodologies were reviewed and analyzed by Martínez-Donaire et al. [7].

The second fracture mechanism results from the pioneering research work by Embury and Duncan [8] in the late 1970's who showed that cracks in punch stretching can be triggered without previous localized necking. The mechanism of fracture without previous localized necking is also observed in single point incremental forming (SPIF) of sheet metal parts [9] and flanges [10] and it is schematically illustrated in Fig. 1 by means of the strain loading path ODE, which experiences no change in direction after crossing the FLC at point D.

The first part of this paper is focused on the description of two-physically-based methodologies to accurately set the onset of necking and the limit strains that were recently proposed by Martínez-Donaire et al. [5-7]. The first is a time-dependent methodology, and the second is a hybrid methodology based on direct visualization and analysis of displacements at the outer sheet surface during the formability test. The second part of this paper revisits fracture forming limits in the light of fundamental concepts of plastic flow and ductile damage with the purpose of analysing the circumstances under which each crack opening mode will occur. The presentation follows the analytical approach that was recently developed by Isik et al [11] and Martins et al. [12] for characterizing fracture loci of anisotropic metal sheets under plane stress loading conditions. Experimental results give support to the presentation and confirm the existence of two different fracture loci corresponding to crack opening by tension (the fracture forming limit line - FFL) and by in-plane shear (the shear fracture forming limit line - SFFL).

2. Forming limit curve

The FLC provides the principal strain pairs on the sheet surface at the onset of necking. Before the initiation of necking, the distribution of strain depends on the geometry of the forming tools, and the geometry and material of the sheet. However, after the onset of necking, the strain concentrates in an unstable localized region, with a size of the order of the sheet thickness, reducing locally the sheet thickness up to final fracture, while the material outside the necking region stops gradually their strain until it vanishes. Recent publications have provided a number of methods to estimate the conventional FLC by means of a time-dependent analysis of the strains, see for instance Hotz et al. [13] and Wang et al. [14], among others, highlighting the current research and industrial interest in determining accurately the onset of necking. However, none of these approaches is nowadays universally accepted.

The authors have proposed a time-dependent method based on the experimental evidence of the necking initiation and development [7]. It makes use on the temporal analysis of the major strain distribution and its first time derivative ($\dot{\varepsilon}_1$, "major strain rate") for a series of points on the outer sheet surface along a cross section perpendicular to the crack. Fig. 2(a) shows a schema of the time evolution of ε_1 and $\dot{\varepsilon}_1$ at two reference points at the necking zone: the point at the boundary of the instability region (A) and the fracture point (B). The boundary of the necking region (A) is defined by the last two points on either side of the crack that cease to strain and reach a zero strain rate just before the crack appears. The point (B) is identified as the point exhibiting the highest strain evolution. Briefly, the onset of necking is established when the strain rate at point (A) reaches a local maximum ($\dot{\varepsilon}^{A}_{1,\max}$), so the limit strains at necking will correspond to the strain $\varepsilon_{1,\lim}$ and $\varepsilon_{2,\lim}$ at point B at that time (Fig. 2(a)).

A second method can be stablished based on the direct observation and analyses of the displacements of the outer surface of the sheet. Fig. 2(b) shows the evolution in time of the Z-displacement along a perpendicular section to the fracture zone in a conventional Nakazima test. As can be seen, a valley is clearly visible at the last stages of the forming process allowing to follow the necking process. Fig. 2(b) depicts schematically the expected Z-displacement referred above at different times, where t_1 denotes a time far from necking and t_4 denotes a time just before fracture. For times far from the failure (e.g. t_1), the surface of the sheet deforms by following to the curvature imposed by the punch. Later, this curve begins to flatten in a certain region (e.g. t_2), developing a necking valley which progressively deepens until the sheet fractures. The instant when outer surface becomes flat indicates that the sheet begins to deform locally and independently of the curvature imposed by the tool. This instant (t_3) is identified as the onset of necking ($t_{necking} = t_3$ in Fig. 2(b)). This flattening process can be easily identified by calculating the first spatial derivative of the Z-displacement (see Fig. 2(b)). So, the onset of necking corresponds graphically to a local change in the slope at the failure zone comparing to the slope of the neighbouring points. Particularly, for Nakazima tests, the plastic instability begins when this slope remains locally constant. As before, the limit strains can be obtained from their corresponding principal strain curves at the fracture point at a time equal to $t_{necking}$ [7].

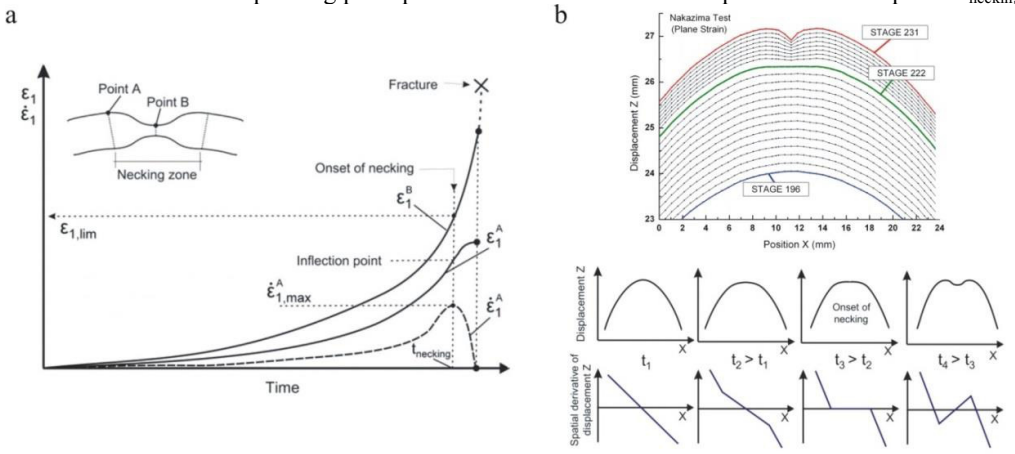

Fig. 2. (a) Graphical scheme of the developed time-dependent methodology; (b) Z-displacement at different stages along a perpendicular section to the failure region in a Nakazima test (top) and expected evolution in time of the Z-displacement profile and its spatial derivative (bottom).

This method, referred in the literature as flat-valley method, can be classified as time-position dependent method, since it depends on both the time and the position evolution of displacements at the outer surface of the sheet around the fracture zone.

Finally, it should be remarked that both methodologies presented above are local, that is, they focus on the evaluation of variables (strains, displacements, etc.) near the failure zone, no matter about the specimen geometry or testing conditions. Therefore, they can be applied not only to near pure stretching conditions, e.g. Nakazima or Marciniak test, but also to situations in which exist a non-negligible strain gradient through the thickness or along the sheet surface [7], e.g. in stretching processes with small-radius punches, stamping processes with high-curvature dies, etc.

3. Fracture limits

At the operating temperatures and rates of loading that are typical of real sheet metal forming processes, fracture usually occurs as ductile fracture, rarely as brittle fracture, in two different opening modes: (i) tensile and (ii) in-plane shear (respectively the same as modes I and II of fracture mechanics).

3.1. Mode I – tensile fracture

Irrespective of the initial loading history before necking, tensile fracture occurs approximately at a constant through-thickness true strain ε_{3f} corresponding to a constant percentage of the reduction in thickness at fracture R_f given by $(t_0 - t_f)/t_0$ where, t_0 is the initial thickness of the sheet and t_f is the thickness at fracture. The reduction in thickness at fracture R_f and ε_{3f} are related by $\varepsilon_{3f} = \ln(1 - R_f)$.

Owing to constancy of volume $\varepsilon_{1f} + \varepsilon_{2f} + \varepsilon_{3f} = 0$ during plastic flow, it follows that the FFL is a straight line falling from left to right with slope '-1' in the principal strain space (refer to Fig. 3(a) where lines of constant R_f are shown). Fig. 3(a) also presents two proportional loading paths (OC and OF) corresponding to uniaxial tension and equal biaxial stretching that fail by fracture at C and F, respectively. For the purpose of simplifying the presentation, both loading paths are taken as linear up to the onset of fracture, without experiencing the change in direction towards plane strain conditions that one would expected to occur after crossing the FLC (refer to Fig. 1).

Considering the following modified version of the effective strain fracture criterion $\bar{\varepsilon} = K$ where the non-dimensional weighting function that corrects the accumulated value of the effective strain until fracture $\bar{\varepsilon}_f$ as a function of the strain loading paths is taken as the stress triaxiality ratio $g = \sigma_H / \bar{\sigma}$ of the hydrostatic σ_H and effective $\bar{\sigma}$ stresses, it is possible to write the following damage criterion:

$$D_{crit} = \int_0^{\bar{\varepsilon}_f} \frac{\sigma_H}{\bar{\sigma}} d\bar{\varepsilon} \tag{1}$$

This criterion is related to the original work of McClintock [15] and its critical value $D_{crit} \propto \ln(l/d)$ may be formulated in terms of the microstructural void parameters that relate the inter-hole l (inter-particle inclusion) spacing and the average diameter d of the holes (particles) (Fig. 3(a)) [16].

Martins et al. [12] showed that by using the constitutive equations associated to Hill's 48 anisotropic yield criterion and assuming rotational symmetry anisotropy $r_\alpha = r = \bar{r}$, where $\bar{r}$ is the normal anisotropy, it is possible to rewrite equation (1) as a function of the major and minor in-plane strains $(\varepsilon_{1f}, \varepsilon_{2f})$ at the onset of fracture:

$$D_{crit} = \int_0^{\varepsilon_{1f}} \frac{(1+r)}{3}\left(\frac{\beta+1}{\beta}\right) d\varepsilon_1 = \frac{(1+r)}{3}\left(\varepsilon_{1f} + \varepsilon_{2f}\right) \tag{2}$$

where $\beta = d\varepsilon_1 / d\varepsilon_2$ is the slope of a general proportional strain path. It follows from equation (2) that the critical value of the damage criterion D_{crit} also defines a straight line with slope '-1' falling from left to right in close agreement with the FFL and the condition of critical reduction of thickness at fracture.

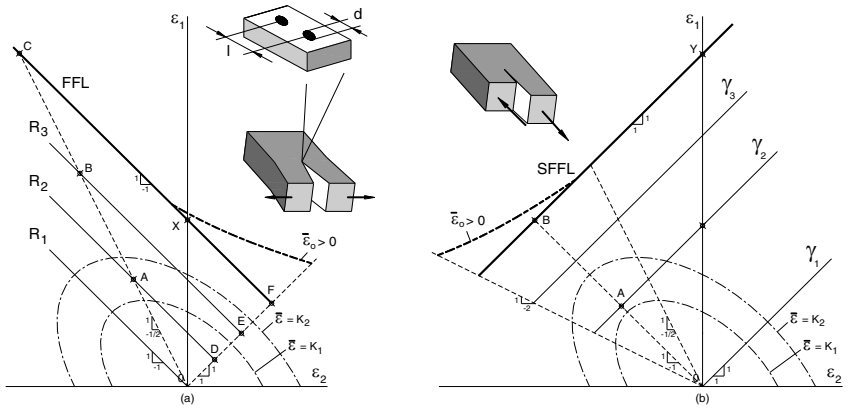

Fig. 3. Schematic representation of the: (a) fracture forming limit line (FFL); (b) in-plane shear fracture forming limit line (SFFL) in the principal strain space.

Three additional conclusions are extracted from equation (2). Firstly, the integrand has the form $(A+B/\beta)$, implying that the damage function for a constant strain ratio β, is independent of loading path history. This occurrence is discussed by Atkins and Mai [16] and justifies the reason why strain loading paths in Fig. 3(a) were assumed as linear. Secondly, if the lower limit of the integral in equation (2) is $\bar{\varepsilon}_0$ rather than zero, corresponding to situations where there is a threshold strain $\bar{\varepsilon}_0$ below which damage is not accumulated, the FFL deviates from a straight line and presents the 'upward curvature' that is schematically represented by the dashed solid line in Fig. 3(a) [12]. Thirdly, combining the relation between the FFL and fracture toughness in mode I that was originally proposed by Muscat-Fenech et al. [17] with above mentioned conclusions regarding the critical reduction in thickness R_f and the critical ductile damage D_{crit} being constant and independent from deformation history up to fracture, it follows that the FFL is a material property in contrast to the FLC that depends on the strain loading path.

3.2. Mode II – shear fracture

In what regards crack opening by in-plane shear (mode II of fracture mechanics), it is important to understand that straight lines γ_1, γ_2 and γ_3 rising from left to right and corresponding to maximum values of the in-plane distortion γ_{12} in the Mohr's circle of strains have slope '+1' and are perpendicular to the FFL (Fig. 3(b)). In-plane distortions γ_{12} (hereafter designated as 'γ') are caused by in-plane shear stresses τ_{12} (hereafter designated as 'τ') and, therefore, it is likely that the in-plane shear fracture limiting locus (SFFL) will coincide with a straight line of slope equal to '+1', in which the major and minor in-plane strains and distortions take critical values at fracture, $\varepsilon_{1f}-\varepsilon_{2f}=\gamma_f$, where, $\gamma_f = Y$ (Fig. 3(b)).

Thus, if the weighting function that corrects the accumulated value of the effective strain until fracture $\bar{\varepsilon}_f$ as a function of the strain loading paths is taken as the in-plane shear stress ratio $g=\tau/\bar{\sigma}$ instead of the stress triaxiality ratio $g=\sigma_H/\bar{\sigma}$ it is possible to define the following damage criterion [14]:

$$D^s_{crit}=\int_0^{\bar{\varepsilon}_f}\frac{\tau}{\bar{\sigma}}d\bar{\varepsilon}=\int_0^{\bar{\varepsilon}_{1f}}\frac{1}{2}\frac{(1+r)}{(1+2r)}\left(\frac{\beta-1}{\beta}\right)d\varepsilon_1=\frac{1}{2}\frac{(1+r)}{(1+2r)}\left(\varepsilon_{1f}-\varepsilon_{2f}\right) \tag{3}$$

The critical values of damage by in-plane shear D^s_{crit} derived from equation (3) are located along a straight line rising from left to right with a slope equal to '+1' in agreement with the condition of critical distortion γ_f along the SFFL. By following a procedure similar to that performed in case of the FFL in case the lower limit of the integral in equation (3) is $\bar{\varepsilon}_0$, it is also possible to conclude that the SFFL deviates from a straight line and presents an 'upward curvature' illustrated by the dashed solid line in Fig. 3(b).

4. Experimental work plan

Giving that the previously described methods for the evaluation of necking and fracture were obtained separately, in the following sections, the experimental application is presented using the materials used in their respective original analysis, which are the most complete set of results available up to now.

The time-dependent and time-position dependent methodologies to detect necking were applied to aluminum alloy 7075-O sheets with 1.6 mm thickness. The experiments were performed with Nakazima tests (100 mm diameter punch) following the ISO 12004-2:2008 standard. The strain history in the outer surface of the test specimens was evaluated by means of digital image correlation (DIC) using the ARAMIS® commercial system.

The work on fracture limits was performed in AA1050-H111 aluminum sheets with 1mm thickness. Experiments were performed with SPIF and double-notched tensile, plane torsion and shear tests. The SPIF tests consisted on forming truncated conical, lobe conical and pyramidal geometries with varying drawing angles up to failure by fracture. The strain loading paths were determined by means of circle grid analysis and DIC technique using ARAMIS® (in the double-notched tests) and the fracture strain pairs were obtained by measuring the sheet thickness before and after failure by fracture at different locations along the crack in order to obtain the 'gauge length' strains.

5. Results and discussion

5.1. Forming limit curve

Fig. 4(a) shows the major strain profile along a section perpendicular to the failure region at several stages for a Nakazima test close to plane strain conditions. Such a section is shown on the major strain contour map at the frame immediately before the specimen fracture. Fig. 4(b) depicts the temporal evolution of major strain for a series of points distributed from the fracture outward along the previous section for the same test.

As can be seen in Fig. 4(b), in the early stages of the test the strain is distributed approximately uniformly over the entire contact region between the punch and the sheet, exhibiting strain curves very similar. However, in the last stages, the curves dramatically separated from each other as a consequence of the development of the necking process. These evolutions are consistent with those shown schematically in Fig. 2(a).

Applying the time-dependent method and the flat-valley method described above, the FLC has been obtained. Fig. 5 compares both predictions with the FLC obtained via the ISO standard. As can be seen, the results of the two developed methods are practically identical for all of the strain paths and very similar to those estimated by ISO 12004- 2:2008. The maximum differences between the three approaches are in the range of 5% to 7%.

As summary, it can be said that the two methodologies (time-dependent and flat valley method) successfully estimate the onset of necking and allow obtaining the conventional FLC as accurate as the standardized method. The main advantages of both methods are their physical meaning, based on the experimental evidence of the necking process, their lack of mathematical complexity and their independence on the type of test.

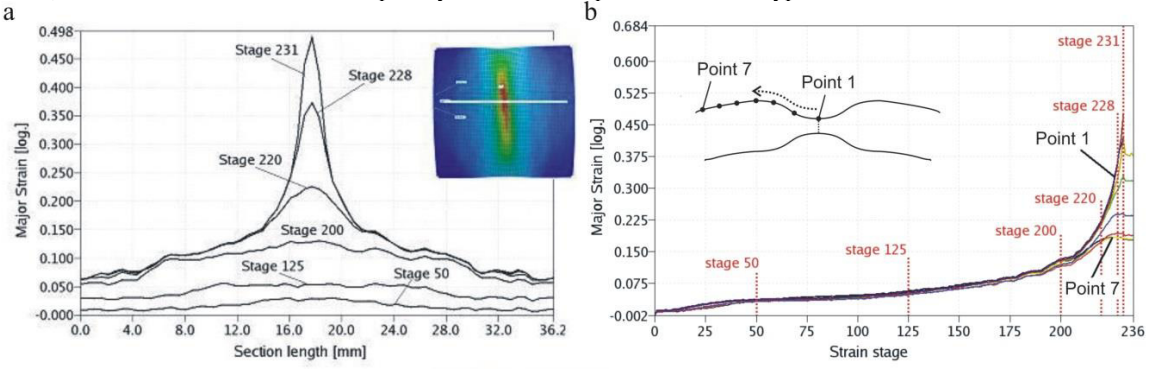

Fig. 4. Experimental data for a Nakazima test in AA7075-O aluminum sheets with 1.6mm thickness: (a) Major true strain distribution along a given section line perpendicular to the crack; (b) major true strain evolution versus the strain stage at different points in that section.

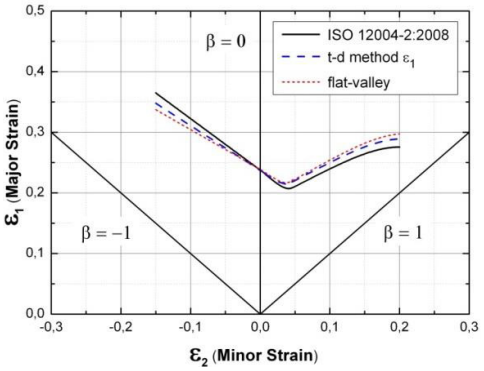

Fig. 5. Forming limit curve of the AA7075-O aluminum sheets with 1.6mm thickness using the ISO 12004- 2:2008 and the proposed methods.

5.2. Fracture limits

Fig. 6 presents the experimental strains at fracture for the AA1050-H111 aluminum sheets with 1 mm thickness that were measured from the experiments performed with SPIF and double-notched tests. The FFL resulting from the double-notched tensile tests and the SPIF tests performed with truncated conical, and pyramidal geometries consists of a straight line falling from left to right with a slope '-0.79'. The SFFL resulting from torsion tests, in-plane shear tests and SPIF tests performed with a truncated lobe conical geometry consists of a straight line rising from left to right with a slope equal to '+1.39':

$$\varepsilon_{1f} + 0.79\varepsilon_{2f} = 1.37 \quad (FFL) \qquad \varepsilon_{1f} - 1.39\varepsilon_{2f} = 2.14 \quad (SFFL) \tag{4}$$

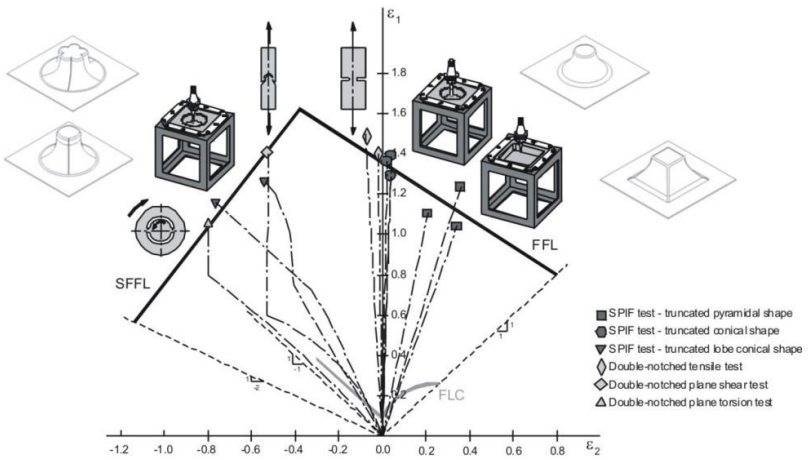

Fig. 6. Values of the major and minor strains at fracture obtained from the experimental tests that were utilized to determine the fracture locus of the AA1050-H111 aluminum sheets with 1mm thickness.

The results are in fair agreement with the theoretical slopes equal to '-1' and '+1' that are predicted by equations (2) and (3) and the angle between the experimental FFL and SFFL is approximately equal to 90 degrees. The fact that the slopes of the FFL and the SFFL are perpendicular, yet they are different from '+1' and '-1' may be attributed to a missing link in the proposed analytical framework that ought to make the slopes dependent on some other effects that are not included in the approach such as, coupled ductile damage, the existence of a threshold

strain $\bar{\varepsilon}_0$ below which damage is not accumulated and the utilization of other yield criteria than Hill's 48 that are more appropriate for modelling plastic flow of aluminum alloys, among others.

6. Conclusions

This paper presents a series of innovative methodologies that were recently developed for the determination of the formability limits by necking and fracture in sheet metal forming. The proposed methods for necking detection (time-dependent and flat valley method) match satisfactorily the results given by ISO 12004-2:2008 standard and may be seen as an alternative approach for the determination of the FLC's. In contrast to ISO standard, the two proposed methodologies are also able to estimate successfully the onset of necking and the limit strains in sheet forming under significant through-thickness strain gradients, which are typical of industrial applications. The local nature of these methods enables its application independently of the type of test to be performed.

A new vision for the formability limits at fracture in sheet metal forming has also been presented. The vision makes use of fundamental plastic flow concepts related to the critical thickness reduction and the critical distortion in sheet metal forming. Fracture loci were characterized by means of a modified version of the effective strain fracture criterion that corrects the values of accumulated damage and, in contrast to alternative methods available in the literature, the proposed approach is exclusively based in sheet metal tests due to the plane-stress plastic flow conditions that are typical of sheet metal forming processes.

Acknowledgements

The authors wish to thank the Spanish Government for its financial support through the research project DPI2012-32913. M.B. Silva and P.A.F. Martins would additionally like to thank Fundação para a Ciência e a Tecnologia of Portugal.

References

[1] H.W. Swift, Plastic instability under plane stress, J. of the Mechanics and Physics of Solids 1 (1952) 1-18.
[2] R. Hill, On discontinuous plastic states with special reference to localized necking in thin sheets, J. of the Mech. and Physics of Solids 1 (1952) 19–30.
[3] Z. Marciniak, Stability of plastic shells under tension with kinematic boundary condition, Arch. Mechaniki Stosorwanej 17 (1965) 577-592.
[4] W. Hotz, J. Timm, Experimental determination of forming limit curves (FLC), 7th Numisheet Conf., Interlaken, 2008, pp. 271-278.
[5] A.J. Martínez-Donaire, C. Vallellano, D. Morales, F.J. García-Lomas, On the experimental detection of necking in stretch-bending tests, American Inst. of Physics 1181 (2009) 500-508.
[6] A.J. Martínez-Donaire, C. Vallellano, D. Morales, F.J. García-Lomas, Experimental detection of necking in stretch-bending conditions: a critical review and new methodology, Steel Research International 81 (2010) 785-788.
[7] A.J. Martínez-Donaire, F.J. García-Lomas, C. Vallellano, New approaches to detect the onset of localized necking in sheets under through-thickness strain gradients, Materials & Design 57 (2014) 135-145.
[8] J.D. Embury, J.L. Duncan, Formability maps, Annual Review of Materials Science 11 (1981) 505-521.
[9] M.B. Silva, M. Skjoedt, A.G. Atkins, N. Bay, P.A.F. Martins, Single point incremental forming & formability/failure diagrams, J. of Strain Analysis for Eng. Design 43 (2008) 15–36.
[10] G. Centeno, M.B. Silva, V.A.M. Cristino, C. Vallellano, P.A.F. Martins, Hole-flanging by incremental sheet forming, Int. J. of Machine Tools & Manufacture 59 (2012) 46–54.
[11] K. Isik, M.B. Silva, A.E. Tekkaya, P.A.F. Martins, Formability limits by fracture in sheet metal forming, J. of Materials Processing Tech. 214 (2014) 1557-1565.
[12] P.A.F. Martins, N. Bay, A.E. Tekkaya, A.G. Atkins, Characterization of fracture loci in metal forming, Int. J. of Mechanical Sciences 83 (2014) 112-123.
[13] W. Hotz , M. Merklein, A. Kuppert, H. Friebe, M. Klein, Time dependent FLC determination – comparison of different algorithms to detect the onset of unstable necking before fracture, Key Engineering Materials 549 (2013) 397-404.
[14] K. Wang, J.E. Carsley, B. He, J. Li, L. Zhang, Measuring forming limit strains with digital image correlation analysis, J. of Materials Processing Tech. 214 (2014) 1120-1130.
[15] F.A. McClintock, A criterion for ductile fracture by the growth of holes, J. of Applied Mechanics - Transactions ASME 35 (1968) 363-371.
[16] A.G. Atkins, Y.W. Mai, Elastic & Plastic Fracture, Chichester, Ellis Horwood, New York, 1985.
[17] C.M. Muscat-Fenech, S. Arndt, A.G. Atkins, The determination of fracture forming limit diagrams from fracture toughness, 4th Int. Conf. Sheet Metal, Twente, The Netherlands, 1996, pp. 249-260.